Figure Legends

Fig. 1. Ro41-5253 decreased susceptibility to HBV infection. (A) Schematic representation of the schedule for treatment of HepaRG cells with compounds and infection with HBV. HepaRG cells were pretreated with compounds for 2 h and then inoculated with HBV in the presence of compounds for 16 h. After washing out the free HBV and compounds, cells were cultured in the absence of compounds for an additional 12 days followed by quantification of secreted HBs protein. Black and dotted bars indicate the interval for treatment and without treatment, respectively. (B) Chemical structure of Ro41-5253. (C-E) HepaRG cells were treated with or without 10 μM Ro41-5253 or 50 U/ml heparin according to the protocol shown in (A) and HBs (C) and HBe (D) antigens in the culture supernatant were measured. Cell viability was also examined by MTT assay (E). (F-H) HBc protein (F), HBV DNAs (G), and cccDNA (H) in the cells according to the protocol shown in (A) were detected by immunofluorescence, real time PCR, and southern blot analysis. Red and blue in (F) show the detection of HBc protein and nuclear staining, respectively. (I, J) Primary human hepatocytes were treated with the indicated compounds and infected with HBV in the presence (I) or absence (J) of PEG8000 according to the protocol shown in (A). The levels of HBV DNA in the cells (I, J) and HBe antigen in the culture supernatant (I) were quantified. The data show the means of three independent experiments. SDs are also shown as error bars. Statistical significance was determined using Student's t-test (*P<0.05, **P<0.01).

Fig. 2. Ro41-5253 decreased HBV entry. (A) HepaRG cells were treated with or without various concentrations (2.5, 5, 10 and 20 μM) of Ro41-5253 followed by HBV infection according to the protocol shown in Fig. 1A. Secreted HBs was detected by ELISA (left). Cell viability was also determined by ELISA (right). (B) Left, Nucleocapsid-associated HBV DNA in HepAD38 cells treated with the indicated compounds (200 nM preS1 peptide, 20 μM Ro41-5253, 1 μM lamivudine, or 1 μM entecavir) for 6 days without tetracycline was quantified by real-time PCR. Middle, HepG2 cells transfected with the reporter plasmids carrying HBV Enhancer I+II, HBV Enh II, or SV40 promoter (Experimental Procedures) were treated with or without Ro41-5253 or HX531 as a positive control to measure the luciferase activity. Right, HepG2.2.15 cells were treated with or without Ro41-5253 or HX531 for 6 days and intracellular HBV RNA was quantified by real time RT-PCR. (C) HepaRG cells were treated with or without indicated compounds (200 nM preS1 peptide, 20 μM Ro41-5253, 1 μM lamivudine, 1 μM entecavir, or 4 μM CsA) followed by HBV infection according to the protocol shown in Fig. 1A. (D) Upper scheme shows the experimental procedure for examining cell surface bound HBV. The cells were pretreated with compounds (50 U/ml heparin, 20 μM Ro41-5253, or 1 μM lamivudine) at 37 °C for 24 h and then treated with HBV at 4 °C for 3 h to allow HBV attachment but not internalization into the cells. After removing free virus, cell surface HBV DNA was extracted and quantified by real time PCR. (E) HepaRG cells pretreated with the indicated compounds (1 μM unconjugated preS1 peptide, 20 μM Ro41-5253) for 24 h were treated with 40 nM FITC-conjugated pre-S1 peptide (FITC-preS1) in the presence of compounds at 37 °C for 30 min. Green and blue signals show FITC-preS1 and nuclear staining, respectively. (F) HepaRG cells pretreated with the indicated compounds (50 U/ml heparin, 200 nM preS1 peptide, 100 ng/ml IL-1β, or 20 μM Ro41-5253) for 24 h were used for the HBV infection assay, where HBV inoculated for 16 h in the absence of the compounds.

Fig. 3. Ro41-5253 reduced NTCP expression. (A) HepaRG cells were treated or untreated with 10 and 20 μM Ro41-5253 or 50 U/ml heparin for 12 h and levels of NTCP (upper panel) and actin (lower panel) were examined by western blot analysis. The relative intensities for the bands of NTCP measured by densitometry are shown below the upper panel. (B) Flow cytometric determination of NTCP protein level on the cell surface of primary human hepatocytes treated with 20 μM Ro41-5253 (red) for 24 h or left untreated (blue). The black line indicates the background signal corresponding to the cells untreated with the primary antibody. (C) RT-PCR determination of the mRNA levels for NTCP (upper panel), ASBT (middle panel) and GAPDH (lower panel) in cells treated with 20 μM Ro41-5253 or 0.1% DMSO for 12 h or left untreated. The relative intensities for the bands measured by densitometry are shown below the panels. (D) HepaRG cells were

treated with siRNA against RARα (si-RARα) plus that against RXRα (si-RXRα), that against NTCP (si-NTCP), and a randomized siRNA (si-control) for three days, and then were re-treated with siRNAs for three days. The cells were pretreated with or without Ro41-5253 for 24 h, and then infected with HBV for 16 h. HBs antigen produced from the infected cells were measured at 12 days postinfection.

Fig. 4. RAR could regulate human NTCP (hNTCP) promoter activity. (A) Left, HuS-E/2 cells were transfected for 6 h with a hNTCP reporter construct with -1143/+108 of the hNTCP promoter region cloned upstream of the Gluc gene (upper, phNTCP-Gluc), together with an internal control plasmid expressing secreted alkaline phosphatase (SEAP) (pSEAP). Cells were treated or untreated with various concentrations of Ro41-5253 (5-40 μM) for 48 h. The Gluc and SEAP activities were determined, and the Gluc values normalized by SEAP are shown. Right, HuS-E/2 cells transfected with a reporter construct carrying the herpes simplex virus thymidine kinase promoter (pTK-Rluc) were examined for luciferase activity in the presence or absence of Ro41-5253 (10-40 μM). (B) HuS-E/2 cells transfected with a Fluc-encoding reporter plasmid carrying three tandem repeats of RAR-binding elements (RARE) (upper, pRARE-Fluc) and Rluc-encoding reporter plasmid driven from herpes simplex virus (HSV) thymidine kinase (TK) promoter (pTK-Rluc) were treated with or without 20 μM Ro41-5253 in the presence or absence of an RAR agonist, ATRA 1 μM for 24 h. Relative values for Fluc normalized by Rluc are shown. (C) HuS-E/2 cells transfected with pRARE-Fluc and pTK-Rluc with or without expression plasmids for RARs (RARα, RARβ, or RARγ) and RXRα were treated with (black) or without (white) Ro41-5253 for 48 h. Relative values for Fluc/Rluc are shown. (D) HuS-E/2 cells were cotransfected with phNTCP-Gluc and pSEAP with or without the expression plasmids for RARs (RARα, RARβ, or RARγ) and RXRα, followed by 24 h treatment or no treatment with 20 μM Ro41-5253. Relative Gluc/SEAP values are shown. (E) phNTCP-Gluc and pSEAP were transfected into HuS-E/2 cells together with siRNAs against RARα (si-RARα), RXRα (si-RXRα), si-RARα plus si-RXRα, or randomized siRNA (si-control) for 48 h. Relative Gluc/SEAP values are indicated. Endogenous RARα, RXRα, and actin proteins were detected by western blot analysis (lower panels). (F) mRNA levels for NTCP and GAPDH were detected in differentiated HepaRG cells treated with or without ATRA (0.5 and 1 μM) for 24 h. (G) Protein levels for endogenous NTCP (upper), RARα (middle), and actin (lower, as an internal control) were determined by western blot analysis of differentiated HepaRG, undifferentiated HepaRG, and HepG2 cells.

Fig. 5. RAR directly regulated the activity of hNTCP promoter. (A) HepaRG cells were treated with or without ATRA, Ro41-5253, or a positive control GW4064, which is a FXR agonist, for 24 h. mRNAs for SHP as well as NTCP and GAPDH were detected by RT-PCR. (B) ChIP assay was performed as described in Experimental Procedures with Huh7-25 cells transfected with or without an expression plasmid for FLAG-tagged RARα plus that for RXRα in the presence or absence of ATRA stimulation. (C) Left, a schematic representation of hNTCP promoter and the reporter constructs used in this study. hNTCP promoter has five putative RAREs [nt -491 to -479, -368 to -356, -274 to -258, -179 to -167 (gray regions), and -112 to -96 (black regions: GAATCCAGCAGAGGTCA)] in nt -1143 to +108 of hNTCP. The mutant constructs possessing mutations within each putative RAREs and in all of five elements (5-Mut) as well as the wild type construct are shown. Right, relative luciferase activities upon overexpression with or without RARα plus RXRα in the presence or absence of Ro41-5253. (D) A deletion reporter construct carrying the region nt -53 to +108 of the hNTCP upstream of the Gluc gene was used for the reporter assay in the presence or absence of Ro41-5253.

Fig. 6. HBV susceptibility was decreased in RAR-inactivated cells. (A) HuS-E/2 cells were transfected with the pRARE-Fluc and pTK-Rluc for 6 h followed by treatment with or without the indicated compounds 20 mM for 48 h. Relative Fluc values normalized by Rluc are shown. (B, C) HepaRG cells treated with or without the indicated compounds 20 μM were subjected to the HBV infection assay according to the scheme in Fig. 1A. HBs antigen in the culture supernatant was determined by ELISA (B). Cell viability was also quantified by MTT assay (C).

Fig. 7. CD2665 had a stronger anti-HBV activity than Ro41-5253. (A) Chemical structure of CD2665. (B) HepaRG cells treated with or without 1 μM preS1 peptide, 0.1% DMSO, or various concentrations of Ro41-5253 or CD2665 (5, 10 and 20 μM) were subjected to HBV infection according to the protocol shown in Fig. 1A. HBV infection was detected by quantifying the HBs secretion into the culture supernatant by ELISA. The efficiency of HBV infection was monitored by ELISA detection of secreted HBs. (C) HuS-E/2 cells transfected with phNTCP-Gluc and pSEAP were treated with the indicated compounds at 20 μM for 24 h. Relative Gluc/SEAP values are shown. (D) NTCP (upper) and actin proteins as an internal control (lower) were examined by western blot analysis of HepaRG cells treated with or without the indicated compounds at 20 μM.

Fig. 8. CD2665 showed a pan-genotypic anti-HBV activity. (A-E) Primary human hepatocytes were pretreated with or without compounds (50 U/ml heparin, 20 μM CD2665, or 0.1% DMSO) and inoculated with different genotypes of HBV according to the scheme show in Fig. 1A. HBs (A-E) and HBe (A-D) antigen secreted into the culture supernatant was quantified by ELISA. Genotypes A (A), B (B), C (C), D (D), and an HBV carrying mutations (L180M/S202G/M204V) (E) were used as inoculum. (F) HBV(L180M/S202G/M204V) was resistant to nucleoside analogs. HepG2 cells transfected with the expression plasmid for HBV/C-AT (white) or HBV/C-AT(L180M/S202G/M204V) (black) were treated with or without 1 μM ETV, 1 μM LMV, or 0.1% DMSO for 72 h. The cells were lysed and the nucleocapsid-associated HBV DNAs were recovered. Relative values for HBV DNAs are indicated. (G) Continuous RAR inactivation could inhibit HBV spread. Freshly isolated primary human hepatocytes were pretreated with or without indicated compounds (1 μM preS1 peptide, 10 μM Ro41-5253, or 10 μM CD2665) and inoculated with HBV at day 0. After removing free viruses, primary human hepatocytes were cultured in the medium supplemented with the indicated compounds for up to 30 days postinfection. At 12, 18, 24, and 30 days postinfection, HBc protein in the cells (left panels, red), and HBs antigen secreted into the culture supernatant (right graph) were detected by immunofluorescence and ELISA, respectively. Red and blue signals in the left panels show the detection of HBc protein and nucleus, respectively.

Fig. 9. Schematic representation of the mechanism for RAR involvement in the regulation of NTCP expression and HBV infection. Left, RAR/RXR recruits to the promoter region of NTCP and regulates the transcription. The expression of NTCP in the plasma membrane supports HBV infection. Right, RAR antagonists including Ro41-5253 and CD2665 repress the transcription of NTCP via RAR antagonization, which decreases the expression level of NTCP in the plasma membrane and abolishes the entry of HBV into host cells.

Fig. 1

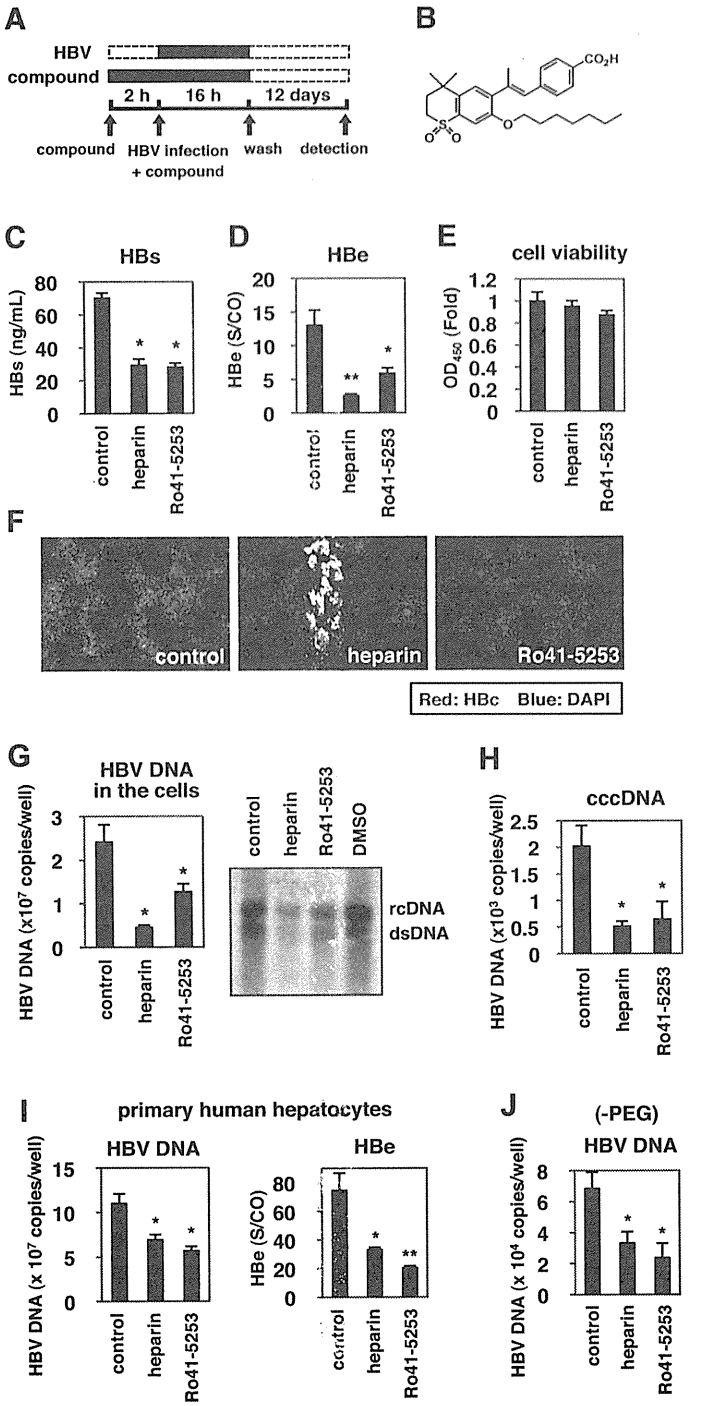

Fig. 2

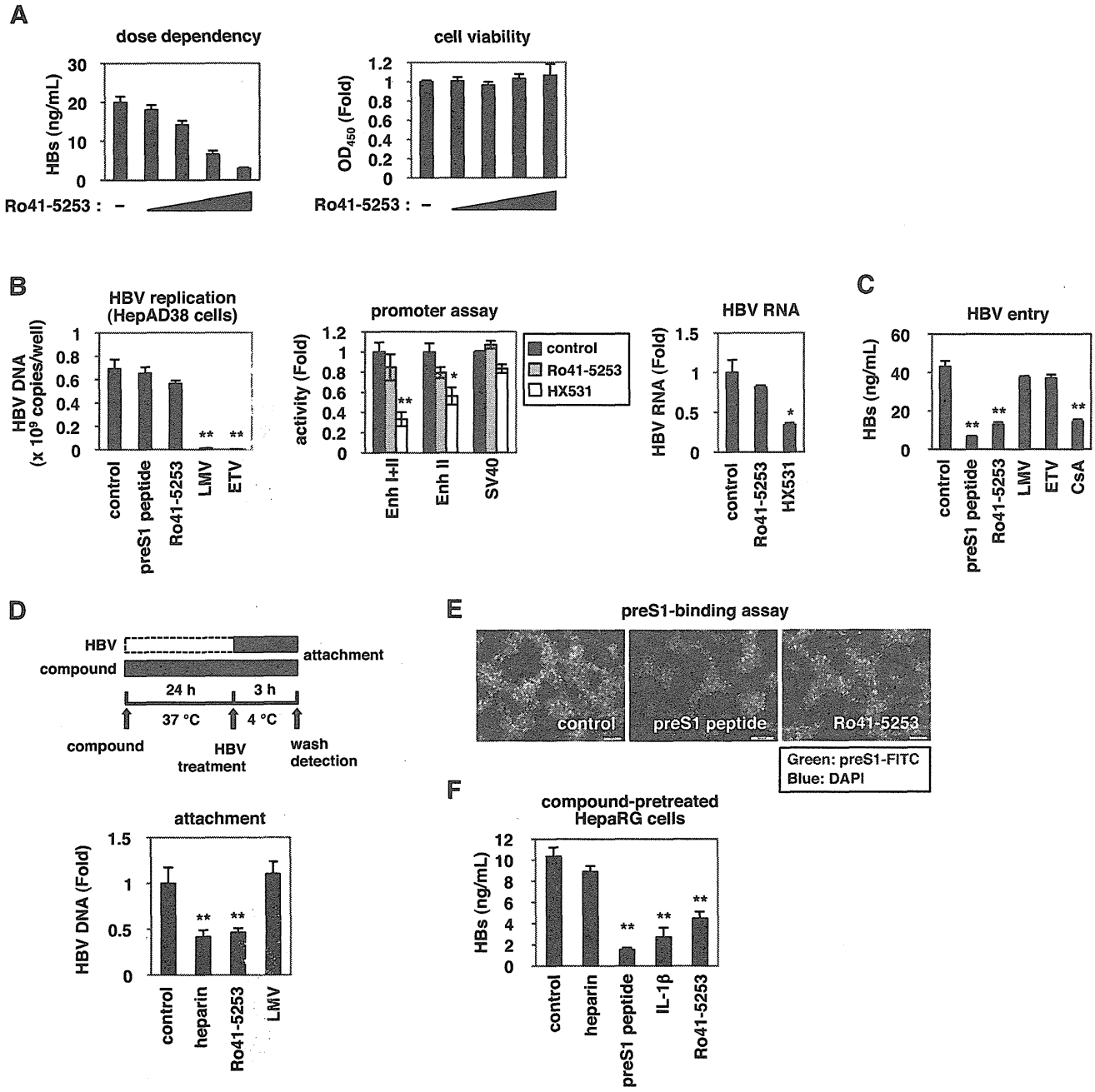

Fig. 3

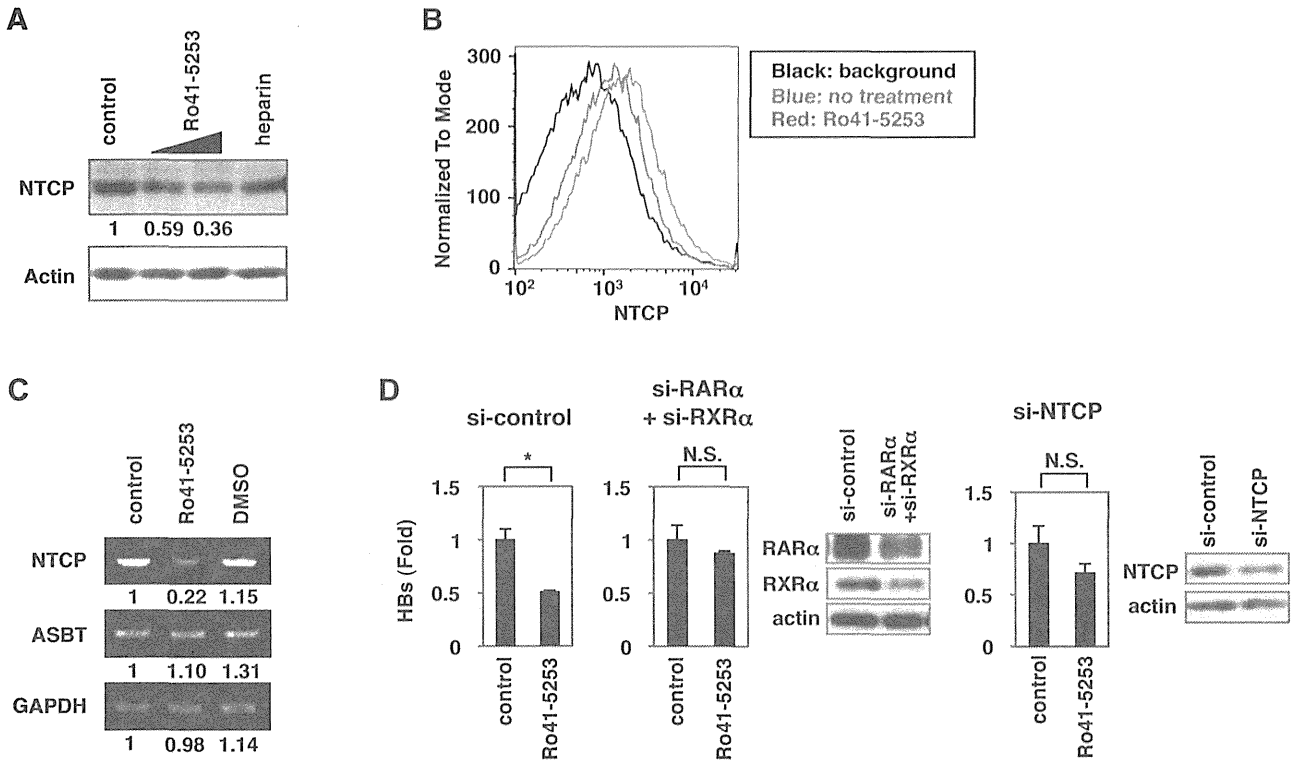

Fig. 4

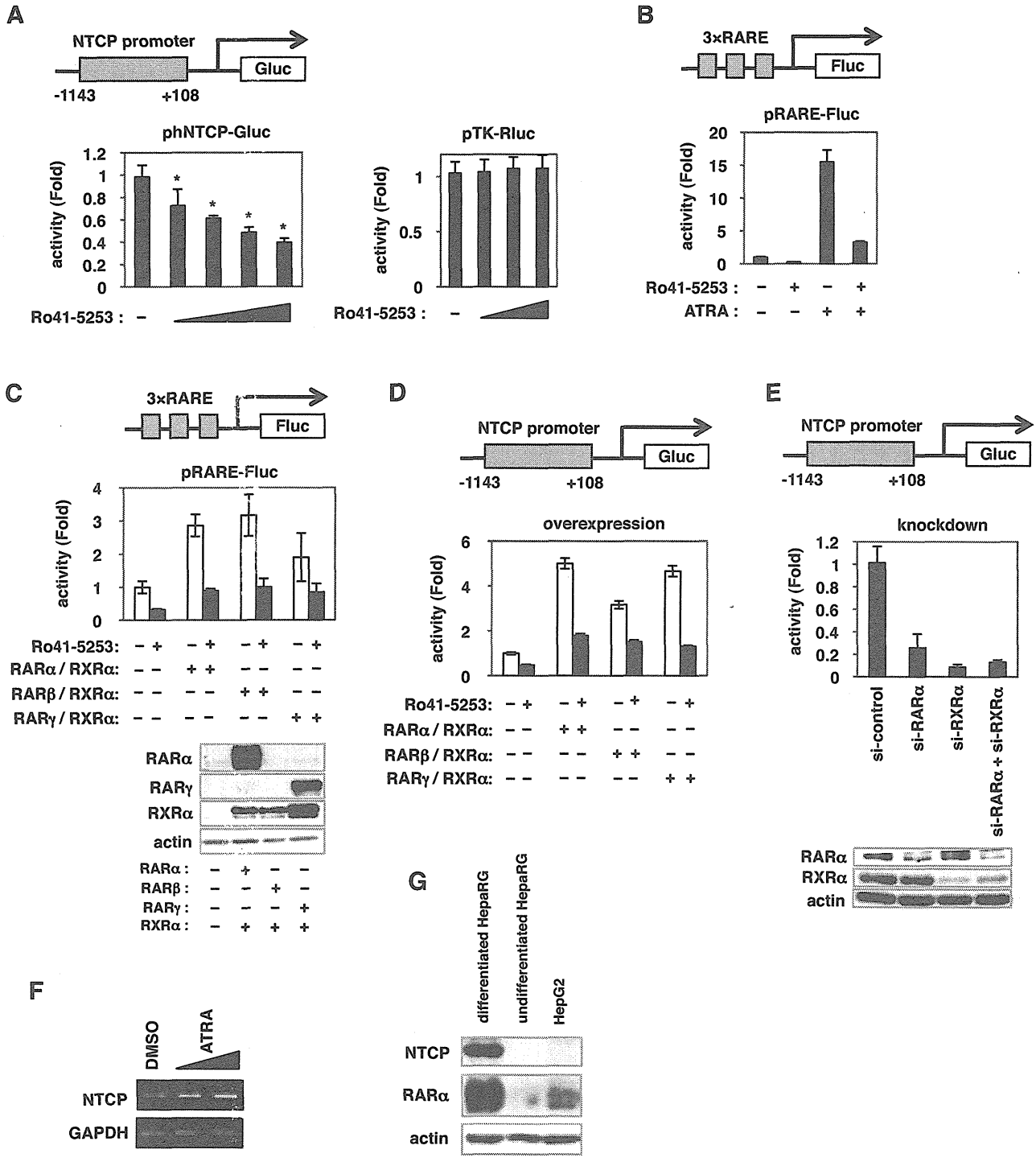

Fig. 5

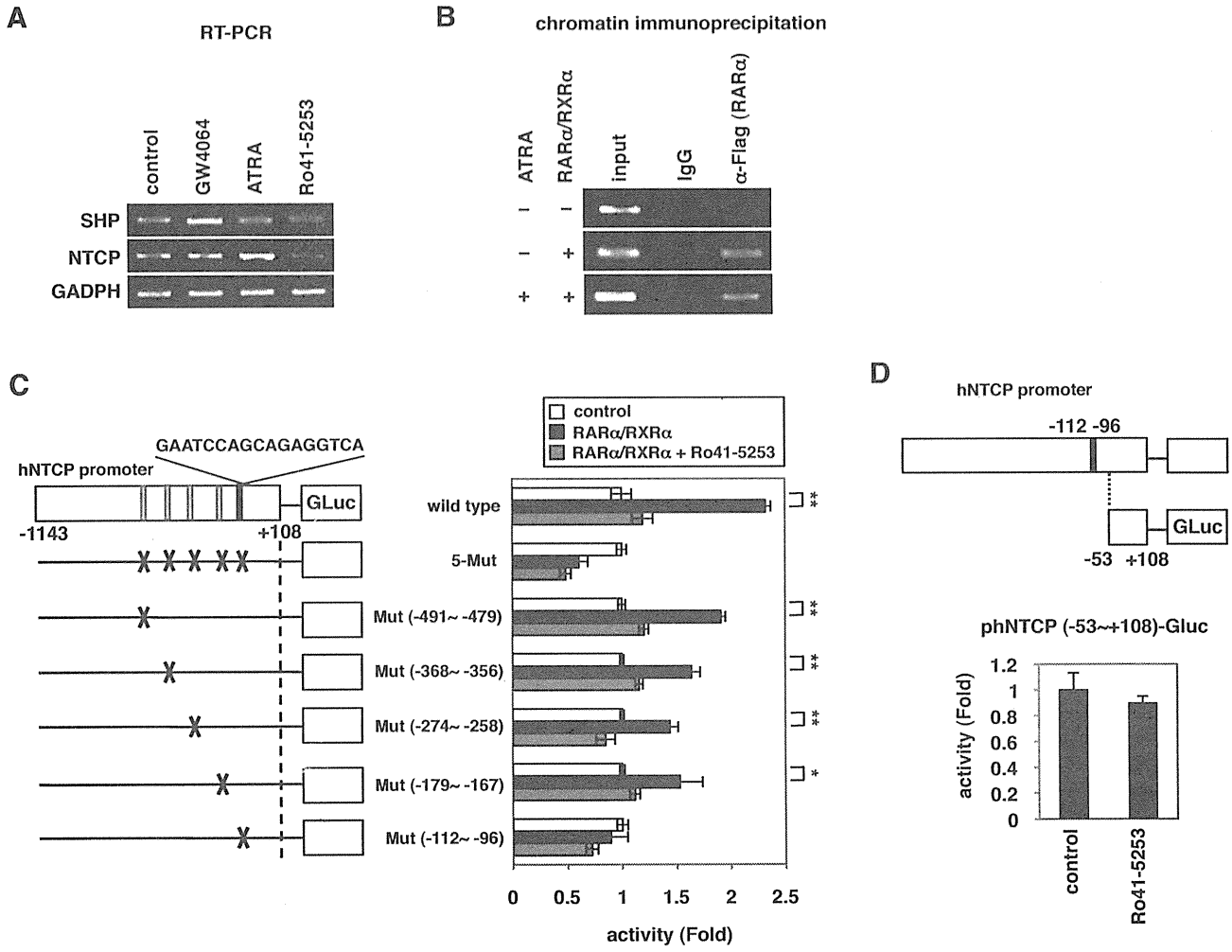
A
RT-PCR
control
GW4064
ATRA
Ro41-5253
SHP
NTCP
GADPH
B
chromatin immunoprecipitation
ATRA
RARα/RXRα
input
IgG
α-Flag (RARα)
C
GAATCCAGCAGAGGTCA
hNTCP promoter
GLuc
-1143
+108
control
RARα/RXRα
RARα/RXRα + Ro41-5253
wild type
5-Mut
Mut (-491~ -479)
Mut (-368~ -356)
Mut (-274~ -258)
Mut (-179~ -167)
Mut (-112~ -96)
**
**
**
**
*
0
0.5
1
1.5
2
2.5
activity (Fold)
D
hNTCP promoter
-112 -96
GLuc
-53 +108
phNTCP (-53~+108)-Gluc
activity (Fold)
1.2
1
0.8
0.6
0.4
0.2
0
control
Ro41-5253

Fig. 6

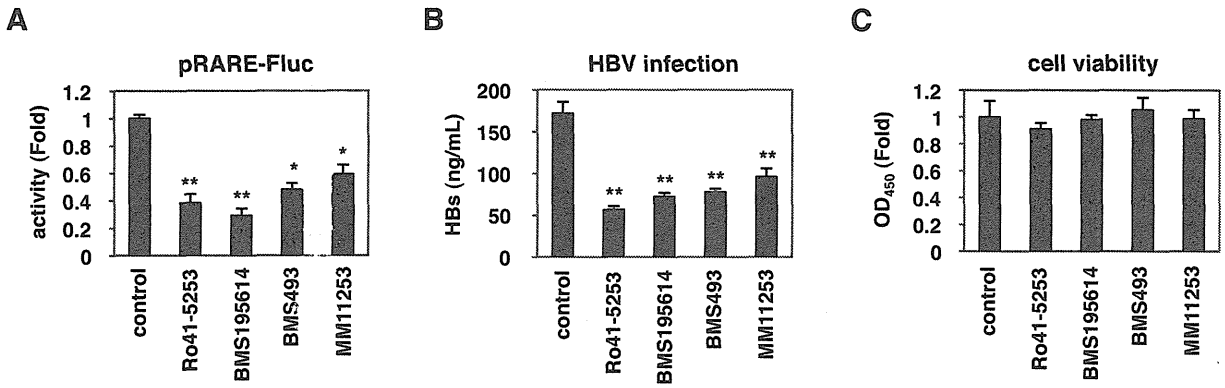
A
pRARE-Fluc
activity (Fold)
1.2
1
0.8
0.6
0.4
0.2
0
control
Ro41-5253
BMS195614
BMS493
MM11253
B
HBV infection
HBs (ng/mL)
200
150
100
50
0
C
cell viability
OD450 (Fold)

Fig. 7

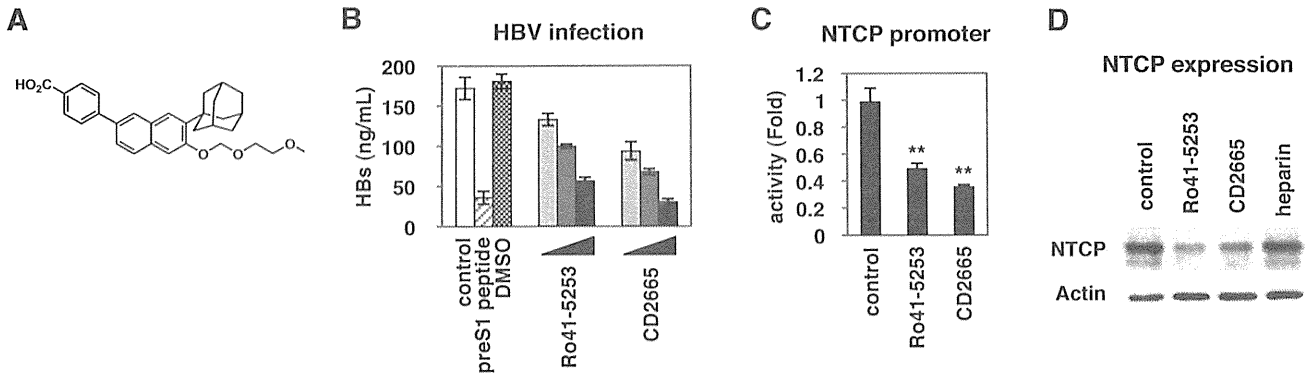
A
HO2C
B
HBV infection
HBs (ng/mL)
200
150
100
50
0
control
preS1 peptide
DMSO
Ro41-5253
CD2665
C
NTCP promoter
activity (Fold)
1.2
1
0.8
0.6
0.4
0.2
0
**
**
control
Ro41-5253
CD2665
D
NTCP expression
control
Ro41-5253
CD2665
heparin
NTCP
Actin

Fig. 8

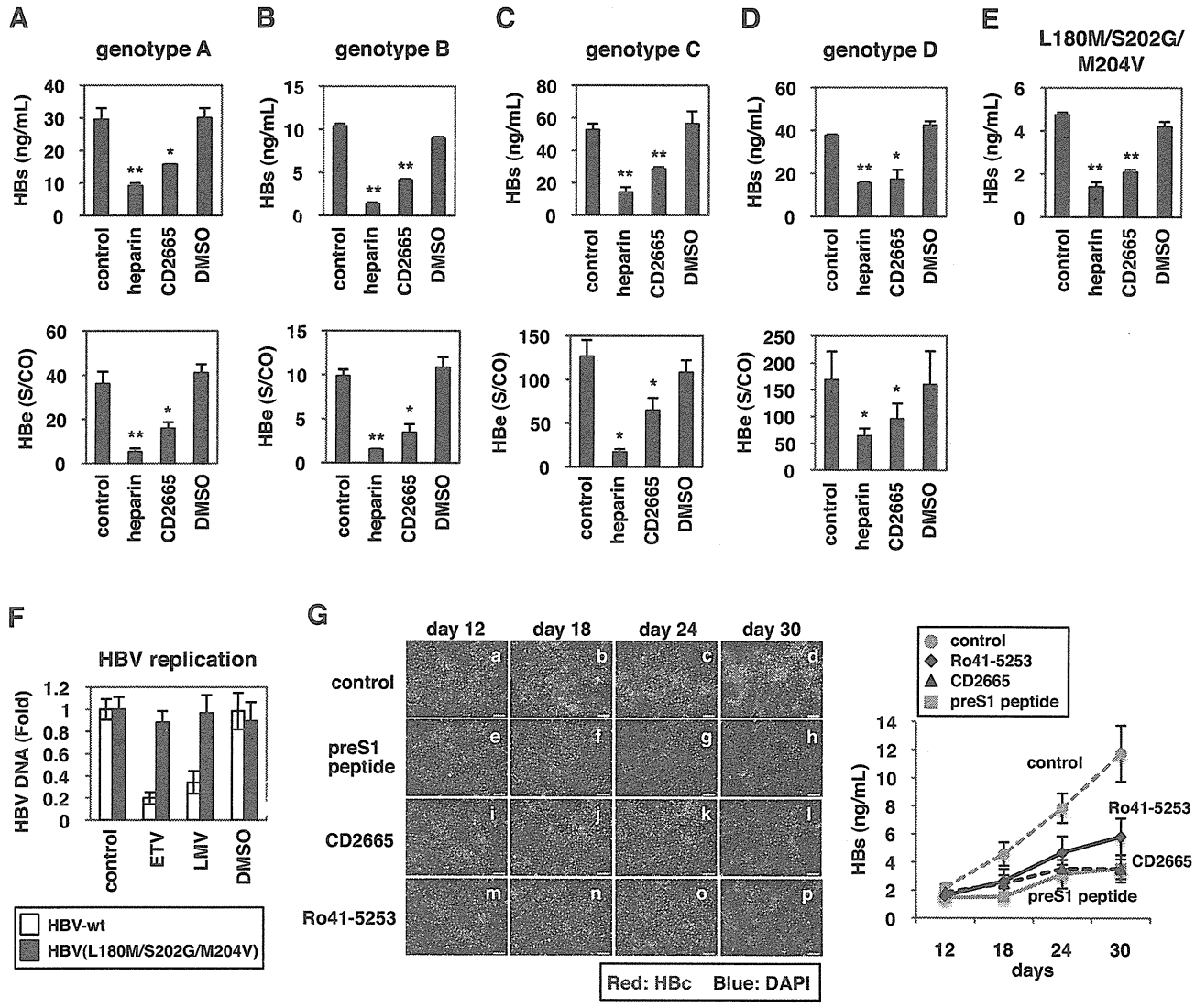
A
genotype A
B
genotype B
C
genotype C
D
genotype D
E
L180M/S202G/
M204V
HBs (ng/mL)
HBe (S/CO)
control
heparin
CD2665
DMSO
F
HBV replication
HBV DNA (Fold)
ETV
LMV
HBV-wt
HBV(L180M/S202G/M204V)
G
day 12
day 18
day 24
day 30
preS1
peptide
Ro41-5253
Red: HBc Blue: DAPI
days

Fig. 9

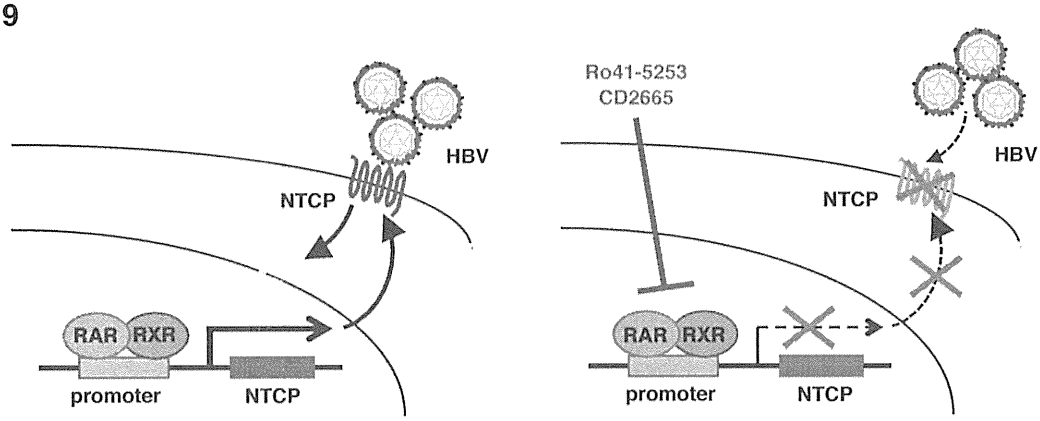
HBV
NTCP
RAR
RXR
promoter
NTCP
Ro41-5253
CD2665
HBV
NTCP
RAR
RXR
promoter
NTCP

Journal of General Virology (2014), 95, 2658–2667 DOI 10.1099/vir.0.068528-0

Alternative endocytosis pathway for productive entry of hepatitis C virus

Mami Matsuda,[1] Ryosuke Suzuki,[1] Chikako Kataoka,[1] Koichi Watashi,[1] Hideki Aizaki,[1] Nobuyuki Kato,[2] Yoshiharu Matsuura,[3] Tetsuro Suzuki[4] and Takaji Wakita[1]

Correspondence
Ryosuke Suzuki
ryosuke@niid.go.jp

[1]Department of Virology II, National Institute of Infectious Diseases, Tokyo, Japan

[2]Department of Tumor Virology, Okayama University Graduate School of Medicine, Dentistry, and Pharmaceutical Sciences, Okayama, Japan

[3]Research Institute for Microbial Diseases, Osaka University, Osaka, Japan

[4]Department of Infectious Diseases, Hamamatsu University School of Medicine, Shizuoka, Japan

Previous studies have shown that hepatitis C virus (HCV) enters human hepatic cells through interaction with a series of cellular receptors, followed by clathrin-mediated, pH-dependent endocytosis. Here, we investigated the mechanisms of HCV entry into multiple HCV-permissive human hepatocyte-derived cells using trans-complemented HCV particles (HCVtcp). Knockdown of CD81 and claudin-1, or treatment with bafilomycin A1, reduced infection in Huh-7 and Huh7.5.1 cells, suggesting that HCV entered both cell types via receptor-mediated, pH-dependent endocytosis. Interestingly, knockdown of the clathrin heavy chain or dynamin-2 (Dyn2), as well as expression of the dominant-negative form of Dyn2, reduced infection of Huh-7 cells with HCVtcp, whereas infectious entry of HCVtcp into Huh7.5.1 cells was not impaired. Infection of Huh7.5.1 cells with culture-derived HCV (HCVcc) via a clathrin-independent pathway was also observed. Knockdown of caveolin-1, ADP-ribosylation factor 6 (Arf6), flotillin, p21-activated kinase 1 (PAK1) and the PAK1 effector C-terminal binding protein 1 of E1A had no inhibitory effects on HCVtcp infection into Huh7.5.1 cells, thus suggesting that the infectious entry pathway of HCV into Huh7.5.1 cells was not caveolae-mediated, or Arf6- and flotillin-mediated endocytosis and macropinocytosis, but rather may have occurred via an undefined endocytic pathway. Further analysis revealed that HCV entry was clathrin- and dynamin-dependent in ORL8c and HepCD81/miR122 cells, but productive entry of HCV was clathrin- and dynamin-independent in Hep3B/miR122 cells. Collectively, these data indicated that HCV entered different target cells through different entry routes.

Received 29 May 2014
Accepted 1 August 2014

INTRODUCTION

Over 170 million people worldwide are chronically infected with hepatitis C virus (HCV), and are at risk of developing chronic hepatitis, cirrhosis and hepatocellular carcinoma (Hoofnagle, 2002). HCV is an enveloped virus belonging to the family *Flaviviridae*. Its genome is an uncapped 9.6 kb positive-stranded RNA consisting of the 5′-UTR, an ORF encoding viral proteins and the 3′-UTR (Suzuki *et al.*, 2007). A precursor polyprotein is further processed into structural proteins (core, E1 and E2), followed by p7 and non-structural (NS) proteins (NS2, NS3, NS4A, NS4B, NS5A and NS5B), by cellular and viral proteases.

Two supplementary figures are available with the online version of this paper.

Host–virus interactions are required during the initial steps of viral infection. Viruses enter the cells by various pathways, such as receptor-mediated endocytosis followed by pH-dependent or -independent fusion from endocytic compartments, or pH-independent fusion at the plasma membrane coupled with receptor-mediated signalling and coordinated disassembly of the actin cortex (Grove & Marsh, 2011). It was reported previously that CD81 (Bartosch *et al.*, 2003; McKeating *et al.*, 2004; Pileri *et al.*, 1998), scavenger receptor class B type I (SR-BI) (Bartosch *et al.*, 2003; Scarselli *et al.*, 2002), claudin-1 (Evans *et al.*, 2007; Liu *et al.*, 2009) and occludin (Benedicto *et al.*, 2009; Liu *et al.*, 2009; Ploss *et al.*, 2009) are critical molecules for HCV entry into cells. Recently, epidermal growth factor receptor and ephrin receptor type A2 were also identified as host cofactors for HCV entry, possibly by modulating interactions between CD81 and claudin-1 (Lupberger *et al.*,

2011). In addition, Niemann–Pick C1-like 1 (NPC1L1) cholesterol absorption receptor has been shown to play a role in HCV entry, probably at the fusion step (Sainz *et al.*, 2012).

Following receptor binding, HCV has been reported to enter cultured cells via clathrin-mediated endocytosis, the most common and best-characterized mode of endocytosis, following membrane fusion in early endosomes (Blanchard *et al.*, 2006; Codran *et al.*, 2006; Coller *et al.*, 2009; Meertens *et al.*, 2006; Trotard *et al.*, 2009) using retrovirus-based HCV pseudoparticles (HCVpp) and cell culture-produced HCV (HCVcc). Early steps in HCV infection, including the role of HCV glycoprotein heterodimers, receptor binding, internalization and pH-dependent endosomal fusion, have been at least in part mimicked by HCVpp. However, as HCVpp are generated in non-hepatic cells such as human embryo kidney 293T cells, it is likely that the cell-derived component(s) of HCVpp differ from those of HCVcc.

In the present study, we readdressed the HCV endocytosis pathway using trans-complemented HCV particles (HCVtcp) (Suzuki *et al.*, 2012), of which the packaged genome is a subgenomic replicon. HCVtcp, generated in Huh-7 or its derivative cell lines with two plasmids, are infectious, but support only single-round infection, thereby allowing us to examine infectious viral entry without the influence of reinfection. In addition, HCVtcp is useful for quantifying productive infection by measuring luciferase activity. Furthermore, it has been shown that the HCVtcp system is more relevant as a model of HCV infection than HCVpp (Suzuki *et al.*, 2012). Our results demonstrated conclusively that, in addition to the clathrin-mediated endocytosis pathway, HCV was capable of utilizing the clathrin- and dynamin-independent pathways for infectious entry of HCV into human liver-derived cells.

RESULTS

HCV entry depends on receptor-mediated, pH-dependent endocytosis

HCV has been shown to enter permissive cells through clathrin-mediated endocytosis and low pH-dependent fusion with endosomes mostly using HCVpp (Codran *et al.*, 2006; Meertens *et al.*, 2006; Trotard *et al.*, 2009), although some researchers have used HCVcc with limited cell lines (Blanchard *et al.*, 2006; Coller *et al.*, 2009). However, several distinct characteristics between HCVpp and HCVcc have recently been revealed with regard to morphogenesis and entry steps (Helle *et al.*, 2010; Sainz *et al.*, 2012; Suzuki *et al.*, 2012; Vieyres *et al.*, 2010). Therefore, in this study, we used HCVtcp, which exhibit similar characteristics to HCVcc when compared with HCVpp and support single-round infection (Suzuki *et al.*, 2012).

Initially, to determine whether receptor candidates such as CD81, claudin-1, occludin and SR-BI are essential for HCV entry into Huh-7 and Huh7.5.1 cells, we examined the knockdown effect of these molecules on HCVtcp infection. Knockdown of these receptors was confirmed by immunoblotting (Fig. 1a) and FACS analysis (Fig. 1b). It should be noted that the luciferase activity in Huh7.5.1 was approximately four times higher than that in Huh-7 cells when the same amount of inoculum was used for infection (Fig. S1, available in the online Supplementary Material), and knockdown did not affect cell viability (data not shown). Knockdown of CD81 and claudin-1 significantly reduced the infection of Huh-7 and Huh7.5.1 cells with HCVtcp derived from genotype 2a (Fig. 1c). Knockdown of occludin led to a moderate reduction in infection; however, only a marginal effect was observed in SR-BI knockdown in both Huh-7 and Huh7.5.1 cells (Fig. 1c), possibly due to the reduced requirement for SR-BI during virus entry by adaptive mutation in E2 (Grove *et al.*, 2008).

Next, to examine whether HCV entry was pH-dependent, Huh-7 and Huh7.5.1 cells were pretreated with bafilomycin A1, an inhibitor of vacuolar H^+-ATPases that impairs vesicle acidification, and then infected with HCVtcp. At 72 h post-infection, luciferase activity and cell viability were determined. Bafilomycin A1 inhibited HCVtcp infection in a dose-dependent manner without affecting cell viability in both Huh-7 and Huh7.5.1 cells (Fig. 2a, b). We also confirmed that treatment with bafilomycin A1 after HCVtcp infection had a minor effect on luciferase activity (Fig. 2c). These results indicated that the infectious route of HCVtcp into Huh-7 and Huh7.5.1 cells is receptor-mediated and involves pH-dependent endocytosis.

Knockdown of clathrin heavy chain (CHC) or dynamin-2 (Dyn2) reduces HCVtcp infection in Huh-7 cells, but not in Huh7.5.1 cells

Among the known pathways of pH-dependent viral endocytosis, clathrin-mediated dynamin-dependent endocytosis is a major endocytosis pathway. Chlorpromazine, an inhibitor of clathrin-dependent endocytosis, has been commonly used to study clathrin-mediated endocytosis; however, it exerts multiple side-effects on cell function as it targets numerous receptors and intracellular enzymes, and alters plasma membrane characteristics (Sieczkarski & Whittaker, 2002a). Therefore, we examined the HCV endocytosis pathway by knockdown of specific molecules required for the endocytosis pathway. CHC, a major structural protein in clathrin-coated vesicles, and Dyn2, a GTPase essential for clathrin-coated-pit scission from the plasma membrane, play important roles in the clathrin-mediated pathway. Another well-studied model of viral entry is caveolin-mediated endocytosis. The role of dynamin in both clathrin-mediated endocytosis and caveolae-dependent endocytosis has been established (Marsh & Helenius, 2006; Miaczynska & Stenmark, 2008). To examine the endocytosis pathways of HCV, small interfering RNAs (siRNAs) for CHC, Dyn2 and caveolin-1 (Cav1), or scrambled control siRNA, were transfected into Huh-7 or

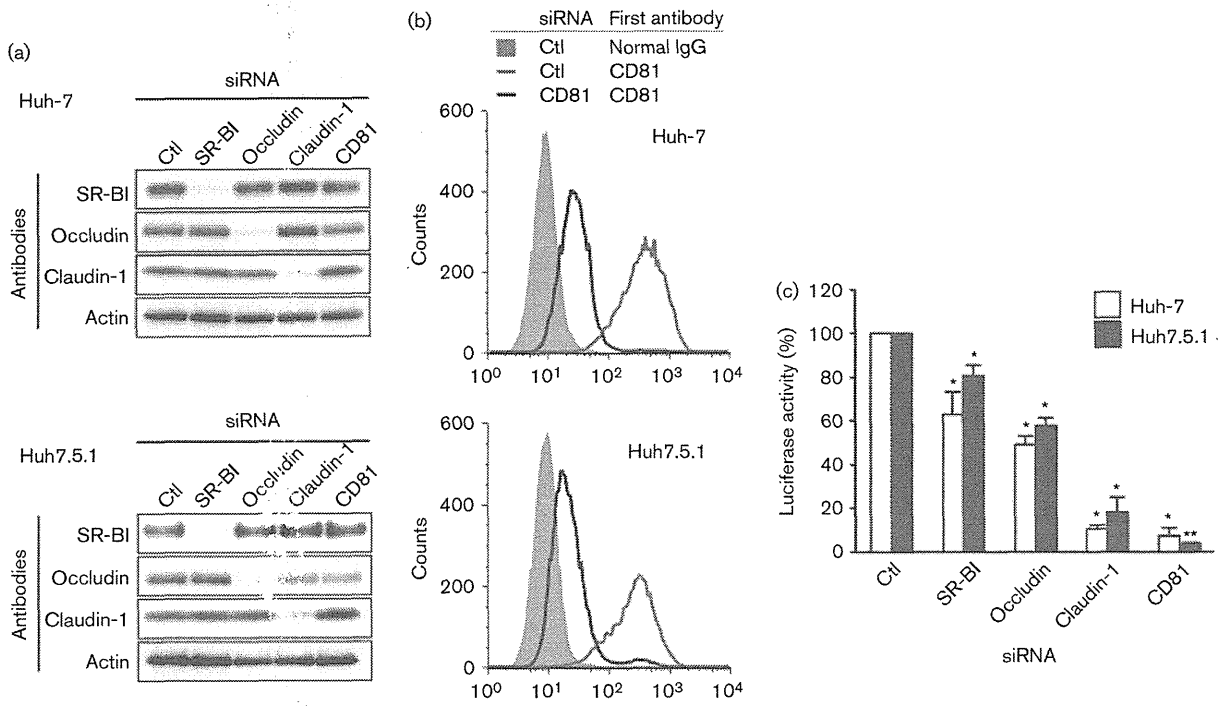

Fig. 1. Knockdown effect of receptor candidate molecules on HCV infection. (a) Huh-7 or Huh7.5.1 cells were transfected with the indicated small interfering RNAs (siRNA), harvested at 48 h post-transfection and the specific knockdown of each protein was verified by immunoblotting. (b) Huh-7 or Huh7.5.1 cells were transfected with CD81 or control siRNAs, harvested at 48 h post-transfection and the cell surface expression of CD81 was verified by FACS analysis. (c) Cells transfected with siRNA were infected with the same amount of HCVtcp at 48 h post-transfection. Firefly luciferase activity in the cells was determined at 72 h post-infection and is expressed relative to the activity with control siRNA transfection. The value for control (Ctl) siRNA was set at 100 %. Data represent the mean ± SD. Statistical differences between controls and each siRNA were evaluated using Student's *t*-test. **P*<0.05, ***P*<0.001 versus control.

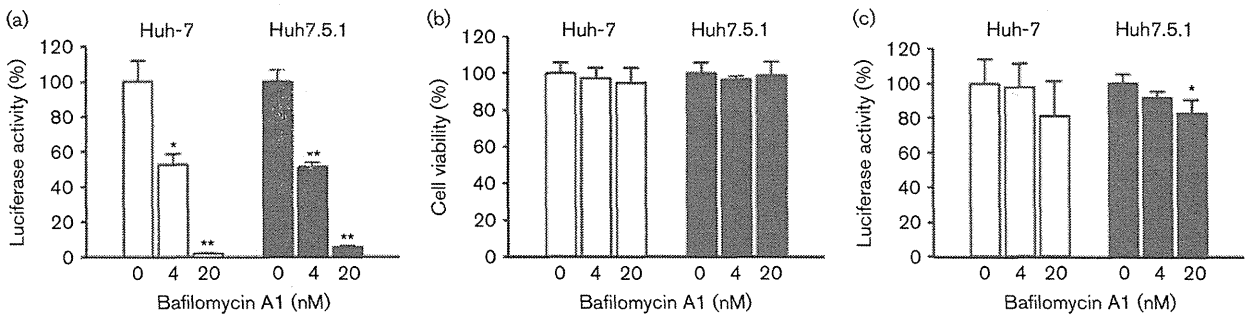

Fig. 2. Role of endosomal low pH in HCV infection. Cells were treated with bafilomycin A1 for 1 h at the indicated concentrations and infected with HCVtcp. (a, b) Luciferase activity (a) and cell viability (b) were determined at 72 h post-infection, and expressed relative to amounts observed in controls. (c) Cells were treated with bafilomycin A1 for 1 h at the indicated concentrations 48 h after HCVtcp infection. Luciferase activity was determined at 10 h post-treatment and expressed relative to amounts observed in controls. Data represent the mean ± SD. Statistical differences between controls and indicated concentrations were evaluated using Student's *t*-test. **P*<0.05, ***P*<0.001 versus control.

Huh7.5.1 cells, followed by infection with HCVtcp. Expression of CHC, Dyn2 and Cav1 was downregulated by transfection of specific siRNAs (Fig. 3a, b), whereas expression of SR-BI, occludin, claudin-1 and CD81 was not reduced (Figs 3a and S2). As indicated in Fig. 3(c), luciferase activity from HCVtcp was significantly reduced by knockdown of CHC and Dyn2 in Huh-7 cells, but not in Huh7.5.1 cells. Knockdown of Cav1 showed no inhibitory effects on HCVtcp entry into either cell line. Dynamin-independent entry in Huh7.5.1 cells was also observed using HCVtcp derived from genotype 1b (data not shown). Knockdown of CHC or Dyn2 also reduced entry of HCVcc in Huh-7 cells, but had no inhibitory effects in Huh7.5.1 (Fig. 3d). To rule out the possibility of effects on CHC and Dyn2 knockdown on viral RNA replication, HCVtcp were also inoculated before siRNA transfection. Luciferase activity was not affected by knockdown of CHC or Dyn2 in either cell line, whereas marked inhibition was observed for phosphatidylinositol 4-kinase (PI4K) (Fig. 3e). These data suggested that HCV entry was clathrin-mediated and dynamin-dependent in Huh-7 cells, but productive entry of HCV was clathrin- and dynamin-independent in Huh7.5.1 cells.

Expression of the dominant-negative form of Dyn2 reduces HCV infection in Huh-7 cells, but not in Huh7.5.1 cells

We also examined the role of dynamin in infectious entry of HCV into Huh-7 and Huh7.5.1 cells by overexpression of the dominant-negative form of Dyn2 (Dyn-K44A), which

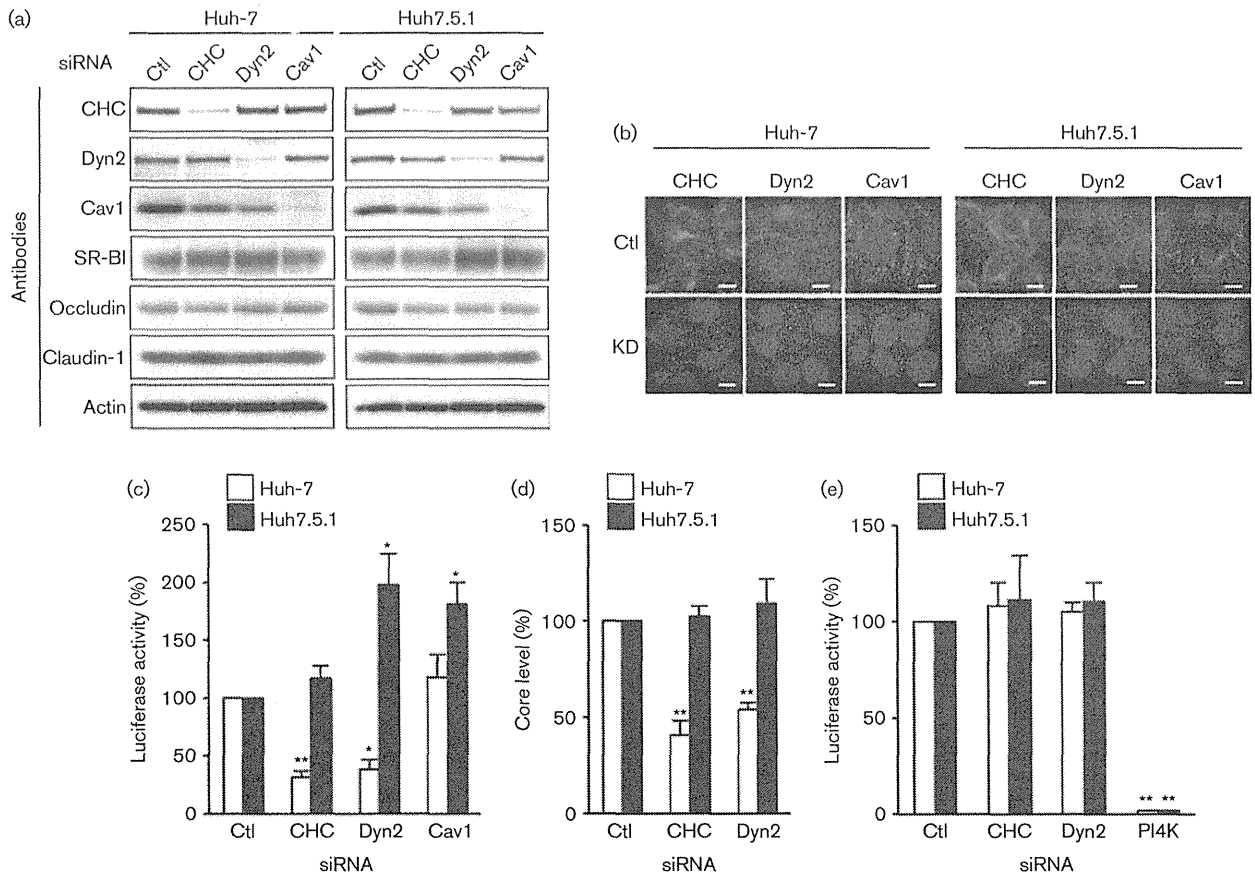

Fig. 3. Effects of CHC, Dyn2 and Cav1 knockdown on HCV infection. (a, b) Huh-7 cells or Huh7.5.1 cells were transfected with the indicated siRNAs and the specific knockdown (KD) of each protein was verified by immunoblotting (a) or immunostaining (b) at 48 h post-transfection. Bar, 50 μm. (c) Cells were transfected with the indicated siRNAs, followed by infection with HCVtcp at 48 h post-transfection. Firefly luciferase activity in the cells was subsequently determined at 3 days post-infection. The value for control (Ctl) siRNA was set at 100 %. Data represent the mean ± SD. (d) Cells were transfected with siRNA, followed by infection with HCVcc at 48 h post-transfection. Intracellular core levels were quantified at 24 h post-infection. The value for control siRNA was set at 100 %. Data represent the mean ± SD. (e) Cells were infected with HCVtcp, followed by transfection with the indicated siRNAs. Luciferase activity in the cells was subsequently determined at 2 days post-transfection. The value for control siRNA was set at 100 %. Data represent the mean ± SD. Statistical differences between controls and each siRNA were evaluated using Student's *t*-test. **P*<0.05, ***P*<0.001 versus control.

has been shown to effectively block clathrin-dependent and caveolar endocytosis (Damke *et al.*, 1995). Expression of haemagglutinin (HA)-tagged Dyn-K44A reduced the number of HCV-infected Huh-7 cells, but not Huh7.5.1 cells, as compared with WT HA-tagged Dyn2 (Dyn-WT), as shown in Fig. 4(a, b). Interestingly, internalization of transferrin, which is known to be mediated by clathrin-dependent endocytosis, was reduced in both Huh-7 and Huh7.5.1 cells expressing Dyn-K44A, whereas cells expressing Dyn-WT showed efficient endocytosis of transferrin (Fig. 4c, d). Collectively, these results suggested that dynamin participated in the internalization of HCV in Huh-7 cells, but was not absolutely required in Huh7.5.1 cells, although transferrin was taken up via dynamin-dependent endocytosis in both Huh-7 and Huh7.5.1 cells.

Flotillin-1 or the GTPase regulator associated with focal adhesion kinase 1 (GRAF1) play no major role during HCV infection of Huh7.5.1 cells

In order to dissect the major endocytosis pathways of HCVtcp in Huh7.5.1 cells, we investigated the role of alternative routes of HCV entry by siRNA knockdown. We silenced essential factors for the clathrin- or dynamin-independent pathways

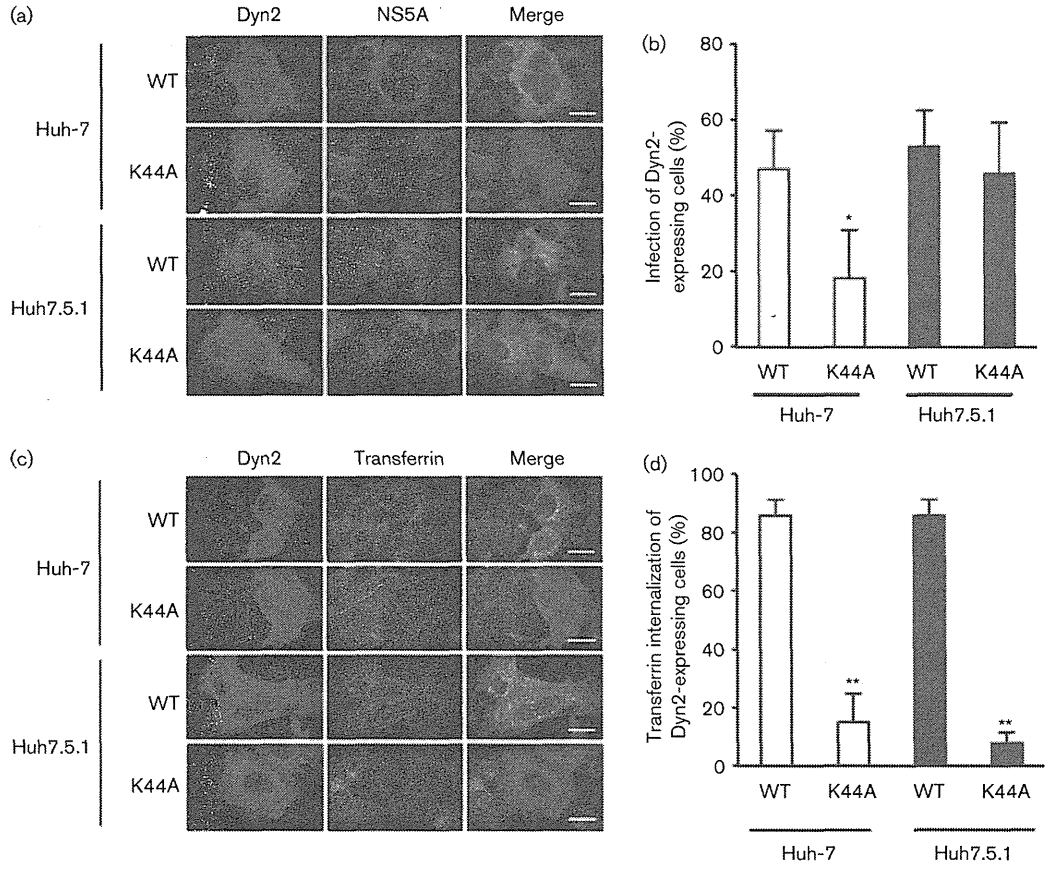

Fig. 4. Dynamin participates in the internalization of HCV in Huh-7 cells, but not in Huh7.5.1 cells. (a) Cells were transfected with HA-tagged WT Dyn2 (Dyn-WT) or dominant-negative Dyn2 (Dyn-K44A) expression plasmids. At 2 days post-transfection, cells were infected with HCVtcp, which possessed a subgenomic replicon without the luciferase gene. After 3 days, cells were fixed and HA-Dyn2 or HCV NS5A stained with anti-HA or anti-NS5A antibodies, respectively. Cell nuclei were counterstained with DAPI. Bar, 100 μm. (b) Data were quantified as the population of HCVtcp-infected cells among HA-positive cells. At least 20 HA-positive cells were evaluated in triplicate experiments. Data represent the mean ± SD. (c) Cells were transfected with HA-tagged Dyn-WT or Dyn-K44A expression plasmids. At 2 days post-transfection, cells were incubated with Alexa Fluor-488 labelled transferrin at 37 °C in a 5 % CO_2 incubator. After 30 min of incubation, cells were washed, fixed and stained with anti-HA antibodies. Cell nuclei were counterstained with DAPI. Bar, 100 μm. (d) Data were quantified as the population of transferrin-internalized cells among HA-positive cells. At least 20 HA-positive cells were evaluated in triplicate experiments. Data represent the mean ± SD. Statistical differences between Dyn-WT and Dyn-K44A were evaluated using Student's *t*-test. **P*<0.05, ***P*<0.001 versus Dyn-WT.

including flotillin-dependent endocytosis, ADP-ribosylation factor 6 (Arf6)-dependent endocytosis, clathrin-independent carrier/glycosylphosphatidylinositol-enriched early endosomal compartment (CLIC/GEEC) endocytic pathway and macropinocytosis in Huh7.5.1 cells. Flotillin-1 and Arf6 are indispensable components of the flotillin and Arf6 pathways, respectively. Knockdown of flotillin-1 or Arf6 had no inhibitory effects on HCVtcp infection in Huh7.5.1 cells (Fig. 5a). The CLIC/GEEC endocytic pathway has recently become better defined and is regulated by the GTPase regulator associated with focal adhesion kinase-1 (GRAF1). However, GRAF1 was not detected in Huh-7 or Huh7.5.1 cells (Fig. 5b); thus, it is unlikely that the CLIC/GEEC pathway was involved in HCV entry in Huh7.5.1 cells. In addition, knockdown of p21-activated kinase 1 (PAK1) and the PAK1 effector C-terminal binding protein 1 of E1A (CtBP1), which play important regulatory roles in the process of macropinocytosis, did not inhibit HCVtcp infection in Huh7.5.1 cells (Fig. 5c). Taken together, these results suggested that the entry of HCVtcp into Huh7.5.1 cells was not mediated mainly by flotillin-dependent endocytosis, Arf6-dependent endocytosis, the CLIC/GEEC endocytic pathway and macropinocytosis.

Clathrin-dependent and -independent pathways for HCV entry in other hepatic cells

We further examined the endocytosis pathways for HCV in non-Huh-7-related human liver-derived cell lines. Three HCVcc permissive hepatocellular carcinoma cell lines, Li23-derived ORL8c (Kato *et al.*, 2009), HepCD81/miR122 cells (HepG2/CD81 cells overexpressing miR122) and Hep3B/miR122 (Kambara *et al.*, 2012), were transfected with siRNA for CHC, Dyn2 or claudin-1, followed by infection with HCVtcp. Immunoblotting was performed in order to confirm knockdown of target proteins (Fig. 6a). Although knockdown of CHC or Dyn2 expression inhibited HCVtcp infection of ORL8c and HepCD81/miR122 cells, HCVtcp infection of Hep3B/miR122 cells was not affected (Fig. 6b), thus suggesting that productive entry of HCV is clathrin- and dynamin-independent in Hep3B/miR122 cells.

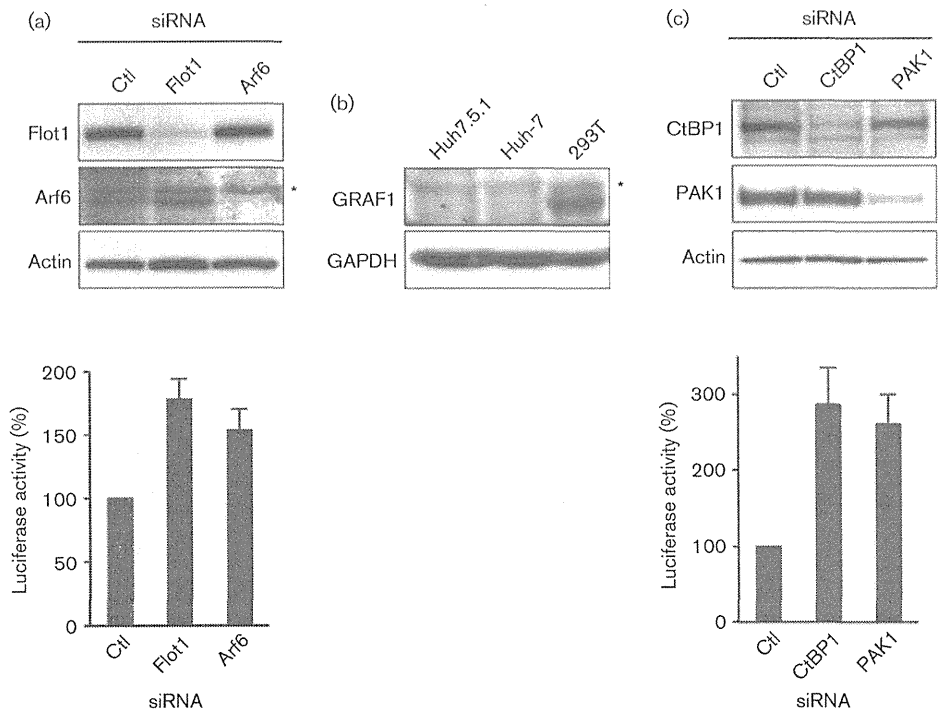

Fig. 5. Role of an alternative endocytosis pathway of HCV in Huh7.5.1 cells. (a) Huh7.5.1 cells were transfected with flotillin-1 (Flot1) or Arf6 siRNAs and specific knockdown of each protein was verified by immunoblotting (upper). Non-specific bands are marked with an asterisk. Cells transfected with siRNA were infected with HCVtcp. Luciferase activity (lower) was determined at 72 h post-infection and expressed relative to the amount observed in control (Ctl) siRNA transfection, Data represent the mean ± SD. (b) Expression of GRAF1 and glyceraldehyde 3-phosphate dehydrogenase (GAPDH) in Huh7.5.1, Huh-7 and 293T cells was analysed by immunoblotting. Non-specific bands are marked with an asterisk. (c) Huh7.5.1 cells were transfected with CtBP1 or PAK1 siRNA and specific knockdown of each protein was verified by immunoblotting (upper). Cells transfected with siRNA were infected with the HCVtcp. Luciferase activity (lower) was determined at 72 h post-infection and expressed relative to the amount observed in control (Ctl) siRNA transfection. Data represent the mean ± SD.

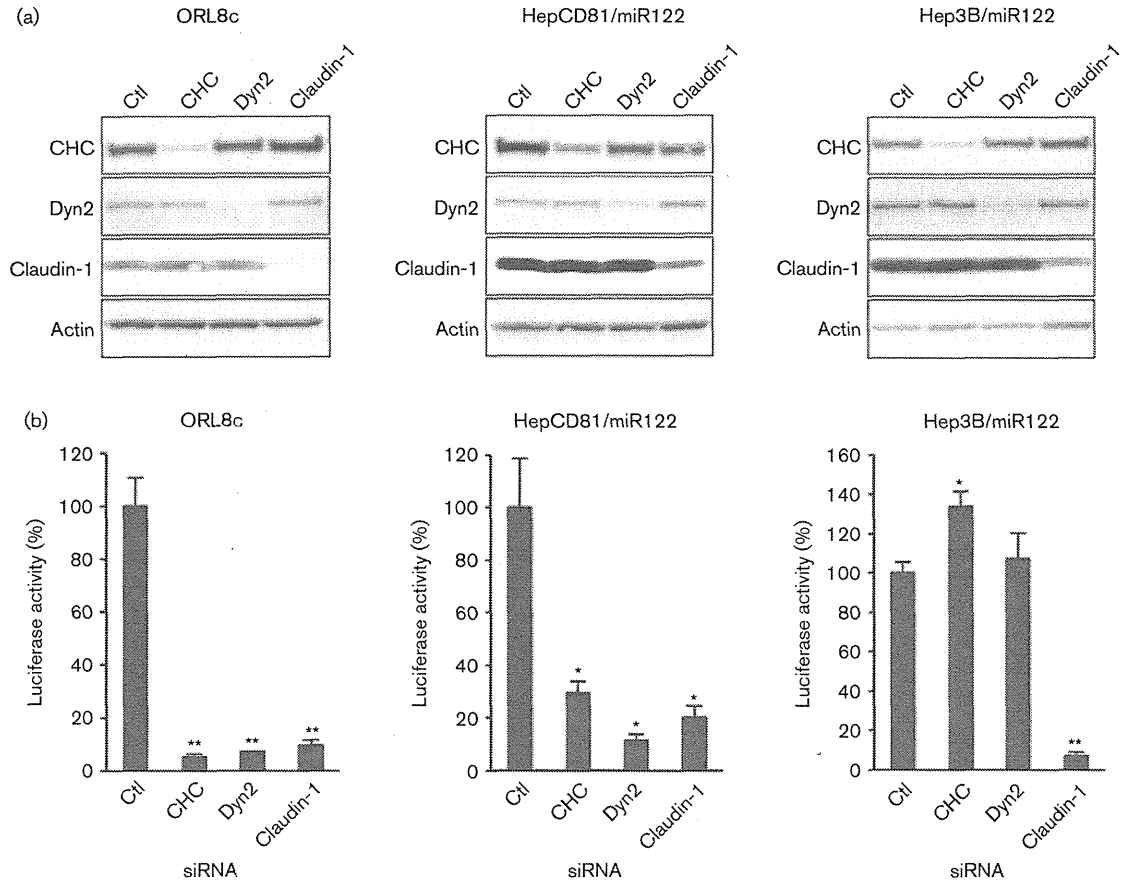

Fig. 6. Clathrin-dependent and -independent pathway of HCV entry in other HCV-permissive cells. The indicated cells were transfected with the indicated siRNAs and then infected with HCVtcp at 48 h post-transfection. (a) Specific knockdown of each protein was verified by immunoblotting. (b) Luciferase activity was determined at 72 h post-infection and expressed relative to the amount observed in the control (Ctl) siRNA transfection. Data represent the mean ± SD. Statistical differences between controls and each siRNA were evaluated using Student's *t*-test. $^{*}P<0.05$, $^{**}P<0.001$ versus control.

In summary, we identified an alternative clathrin- and dynamin-independent entry pathway for HCV in at least two independent cell lines, Huh7.5.1 and Hep3B/miR122 cells, in addition to the previously reported clathrin- and dynamin-dependent pathway. These findings provided clues for understanding the molecular mechanisms of the endocytosis pathway for HCV infection.

DISCUSSION

Many viruses have been shown to utilize a number of different endocytic pathways to productively infect their hosts. Clathrin-dependent endocytosis would appear to be the most commonly used, but it is increasingly clear that a number of clathrin-independent endocytosis pathways are also used by several different viruses (Mercer *et al.*, 2010). In the case of HCV, it has been reported that viral entry is mediated by clathrin-dependent endocytosis (Blanchard *et al.*, 2006; Codran *et al.*, 2006; Coller *et al.*, 2009; Meertens *et al.*, 2006; Trotard *et al.*, 2009). In these papers, HCVpp was used at least in part for analysis of HCV entry pathway. However, recent reports have revealed several different characteristics between HCVpp and HCVcc.

Viral entry has been addressed primarily by pharmacologic inhibitor studies, immunofluorescence and electron microscopy, by transfection with dominant-negative constructs, and more recently by siRNA knockdown. Analysis of endocytosis pathways using pharmacological inhibitors has raised concerns about specificity. For example, chlorpromazine, an inhibitor of clathrin-mediated endocytosis, has been shown to exert multiple side-effects on cell function as it targets numerous receptors and intracellular enzymes, and alters plasma membrane characteristics (Sieczkarski & Whittaker, 2002a). Methods for elucidating the viral endocytosis pathway by co-localization of virus particles with host factor also have limitations. Electron and

fluorescence microscopy, which require a high particle number, do not allow the differentiation of infectious and non-infectious particles. Infectious particles of HCV in the supernatant of infected cells appeared to represent only a small portion of secreted virus particles (Akazawa *et al.*, 2008) and it is unclear whether the viral particles observed by microscopy could lead to productive infection. Therefore, we utilized HCVtcp, which is useful for determining productive entry of the virus without reinfection, and a combination of siRNA knockdown and dominant-negative mutants for analysis of the productive route of infection. Although HCVcc is also utilized in analysis of productive entry, it cannot completely exclude the effects of reinfection by virus produced by infected cells. Reduction of HCVcc infection by knockdown of CHC and Dyn2 was moderate when compared with that of HCVtcp (Fig. 3c, d), thus suggesting slight effects due to reinfection in HCVcc.

The data presented here demonstrate for the first time to our knowledge that HCV is able to enter cells via dynamin-independent endocytosis in addition to the previously described classical clathrin- and dynamin-dependent pathway. First, knockdown of CHC and Dyn2 had no inhibitory effects on HCVtcp and HCVcc entry into Huh7.5.1 cells. Second, overexpression of dominant-negative Dyn2 had no inhibitory effects on HCVtcp in Huh7.5.1 cells. Finally, in addition to Huh7.5.1 cells, Hep3B/miR122 cells were also shown to be infected with HCV via clathrin- and dynamin-independent pathways. We further investigated the role of alternative minor routes of HCV entry into Huh7.5.1 cells; however, the productive endocytosis pathway could not be defined. It should be noted that inhibition of alternative endocytosis routes by siRNA led to an increase of luciferase activity (Figs 3c and 5a, c). This could be explained by the inhibition of a particular endocytosis pathway resulting in a compensatory increase in alternative endocytosis pathways (Damke *et al.*, 1995).

Although we confirmed an alternative endocytosis pathway for the productive entry of HCV, it is not clear why and how the two independent endocytosis pathways operate in different cell lines. SV40 can enter cells via caveolae-dependent (Norkin *et al.*, 2002; Pelkmans *et al.*, 2001) and -independent (Damm *et al.*, 2005) pathways. Influenza virus enters cells via clathrin-mediated endocytosis (Matlin *et al.*, 1981) in addition to non-clathrin-mediated, non-caveola-mediated internalization pathways (Sieczkarski & Whittaker, 2002b). Entry of dengue virus type 2 is clathrin-dependent in HeLa and C6/36 cells (Acosta *et al.*, 2008; Mosso *et al.*, 2008; van der Schaar *et al.*, 2008), and is clathrin-independent in Vero cells (Acosta *et al.*, 2009). Different receptor usage may determine the consequential route of entry. However, we did not observe any differences between Huh-7 and Huh7.5.1 cells in terms of knockdown effects of receptor candidate molecules on HCV infection, as shown in Fig. 1(c), although we cannot exclude the possibility that other undefined receptors are associated with viral entry. Huh7.5.1 cells were established by elimination of the HCV genome from replicon cells derived from Huh-7 cells (Blight *et al.*, 2002; Zhong *et al.*, 2005) and they exhibit more potent replication of HCV than the original Huh-7 cells. Further study showed that the increased permissiveness of cured cells results from a mutation in the retinoic acid-inducible gene I (Sumpter *et al.*, 2005), which impairs IFN signalling. In addition, it has been shown that cured cell lines express higher levels of miR122 than parental cells participating in the efficient propagation of HCVcc (Kambara *et al.*, 2012). As it is unclear whether these changes are the reason for a distinct endocytosis pathway, it will be of interest to explore these associations in further studies.

In conclusion, we confirmed an alternative clathrin-independent endocytosis pathway in HCV-permissive human hepatic-derived cells, in addition to the previously reported clathrin-dependent endocytosis pathway. This paper highlights the fact that clathrin- and dynamin-mediated endocytosis is the main route of HCV entry for Huh-7, HepCD81/miR122 and ORL8c cells, whilst clathrin and dynamin do not play a major role during the productive route of HCV infection in Huh7.5.1 and Hep3B/miR122 cells. Taken together, these studies suggest that different cell entry pathways for HCV infection may be utilized in different cell types, although further studies are necessary in order to understand this phenomenon.

METHODS

Cells. The human hepatocellular carcinoma cell lines Huh-7, Huh7.5.1, Hep3B/miR122 and HepG2/CD81, which overexpressed miR122 (Kambara *et al.*, 2012), were maintained in Dulbecco's modified Eagle's medium (DMEM; Wako Pure Chemical Industries) containing non-essential amino acids, penicillin (100 U ml^{-1}), streptomycin (100 μg ml^{-1}) and 10 % FBS. Li23-derived ORL8c cells (Kato *et al.*, 2009) were maintained in F12 medium and DMEM (1 : 1, v/v) supplemented with 1 % FBS, epidermal growth factor (50 ng ml^{-1}), insulin (10 μg ml^{-1}), hydrocortisone (0.36 μg ml^{-1}), transferrin (5 μg ml^{-1}), linoleic acid (5 μg ml^{-1}), selenium (20 ng ml^{-1}), prolactin (10 ng ml^{-1}), gentamicin (10 μg ml^{-1}), kanamycin monosulfate (0.2 mg ml^{-1}) and fungizone (0.5 μg ml^{-1}). All cell lines were cultured at 37 °C in a 5 % CO_2 incubator.

Preparation of viruses. HCVtcp and HCVcc derived from JFH-1 with adaptive mutations in E2 (N417S), p7 (N765D) and NS2 (Q1012R) were generated as described previously (Suzuki *et al.*, 2012). For HepCD81/miR122 and ORL8c cells, HCVtcp containing the *Gaussia* luciferase (GLuc) reporter gene were used. To do this, plasmid pHH/SGR-JFH1/GLuc/NS3m carrying the bicistronic subgenomic HCV replicon containing the GLuc reporter gene and the NS3 adaptive mutation was constructed by replacement of the firefly luciferase (FLuc) gene of pHH/SGR-Luc containing the NS3 mutation (N1586D) (Suzuki *et al.*, 2012) with the GLuc gene of pCMV-GLuc (NEB).

Plasmids. HA-tagged Dyn2, a dominant-negative Dyn2 (K44A) in which Lys44 was replaced with Ala, was cloned into pcDNA3.1 as described previously (Kataoka *et al.*, 2012).

Gene silencing by siRNA. siRNAs were purchased from Sigma-Aldrich and were introduced into the cells at a final concentration of